Supplementary Information for

Robust second-order topological insulator in 2D van der Waals magnet CrI_3

Xiaorong Zou, Yingxi Bai, Ying Dai, * Baibiao Huang, and Chengwang Niu*

School of Physics, State Key Laboratory of Crystal Materials, Shandong University, Jinan 250100, China

*Corresponding author: daiy60@sina.com (Y.D.); c.niu@sdu.edu.cn (C.N.)

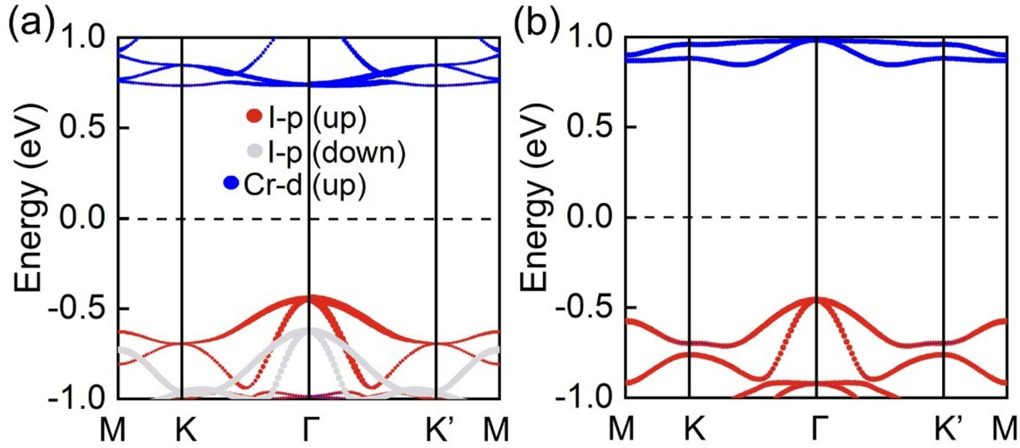

Fig. S1 Band structures of CrI_3 monolayer without SOC for (a) FM ordering and (b) AFM ordering.

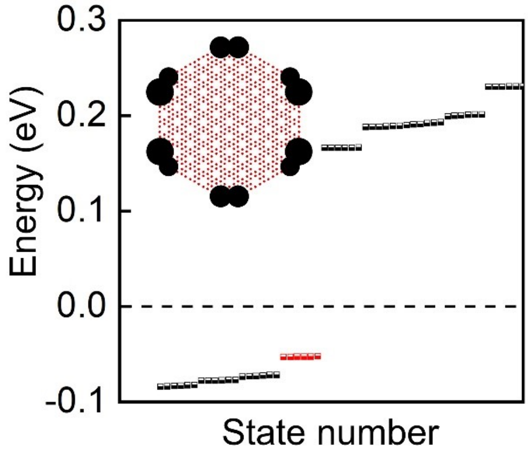

Fig. S2 Energy discrete spectra of hexagonal nanoflake for FM CrI_3 monolayer. Insets show the total charge distribution of the six occupied corner states.

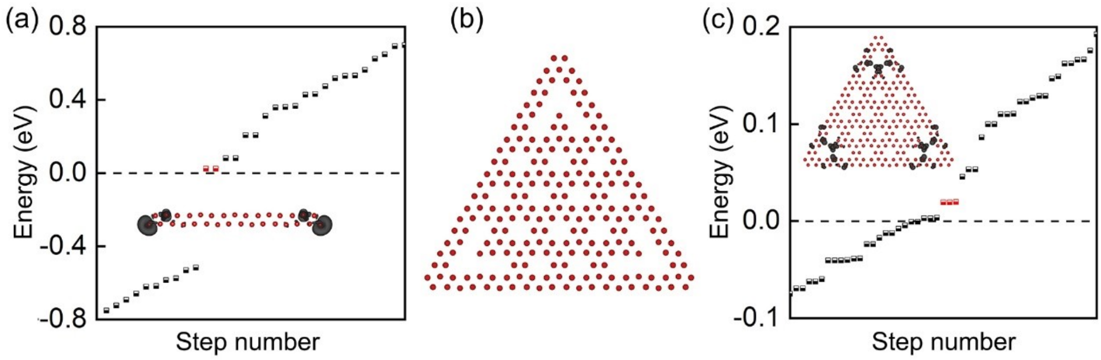

Fig.S3 (a) Energy spectrum of the finite 1D nanostructure, exhibiting two topological end states. Inset is the charge density distribution of the topological end states. (b) Finite nanoflake of CrI_3 containing three point-defects. (c) Energy spectrum of the finite nanoflake, showing the emergence of topological point states located inside the bulk band gap. Insets are charge density distributions of in-gap topological point states.

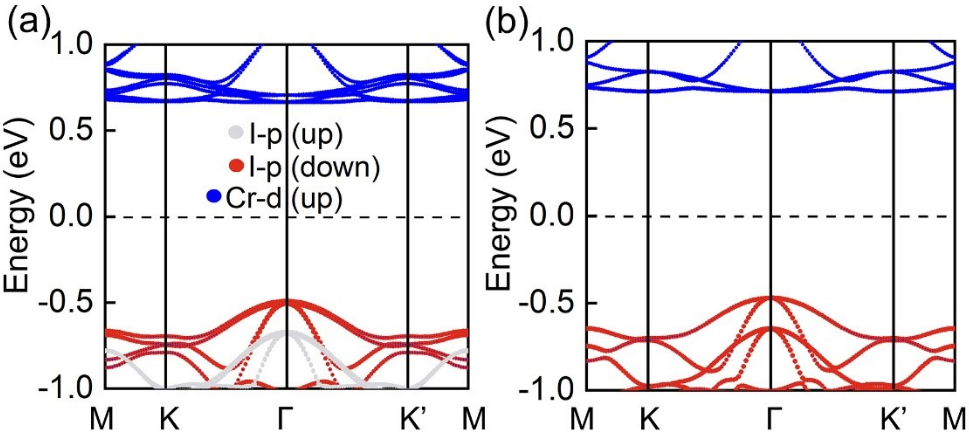

Fig. S4 Band structures of CrI_3 bilayers without SOC for (a) AB stacking and (b) AB' stacking.

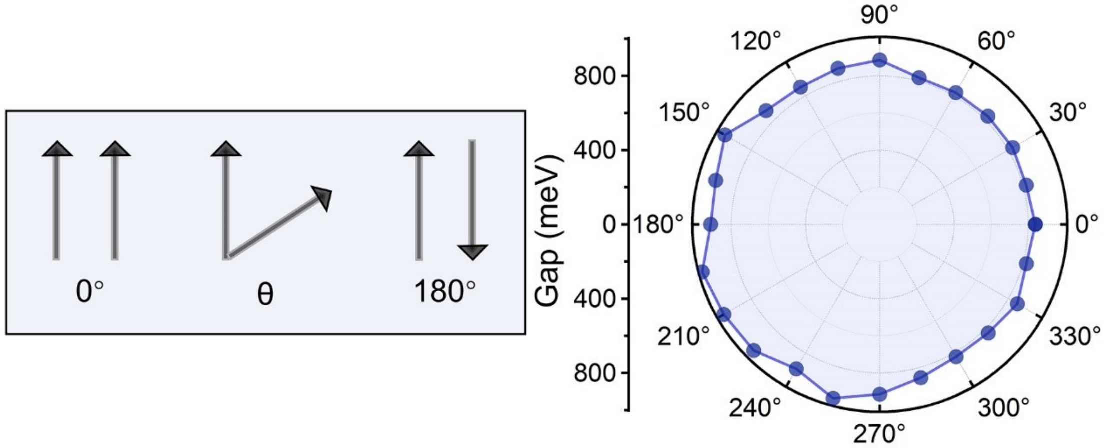

Fig. S5 Evolution of the global band gaps for CrI_3 monolayer with respect to the relative spin orientations θ. There is no band gap closing and reopening process, revealing the robustness of SOTIs against magnetic transition between FM (θ = 0°) and AFM (θ = 180°) orderings.

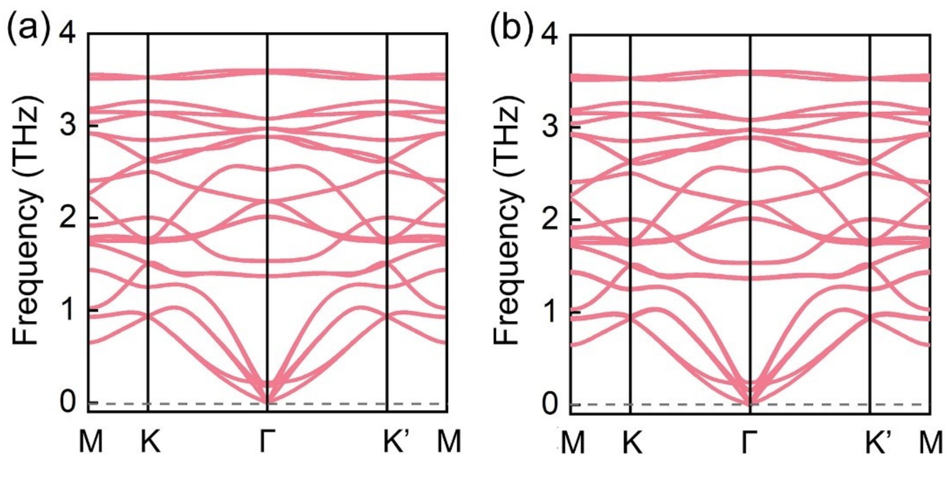

Fig. S6 Phonon spectrums of CrI_3 bilayers for (a) AB stacking and (b) AB' stacking. The absence of imagine frequency in the whole Brillouin zone indicates the dynamical stability.

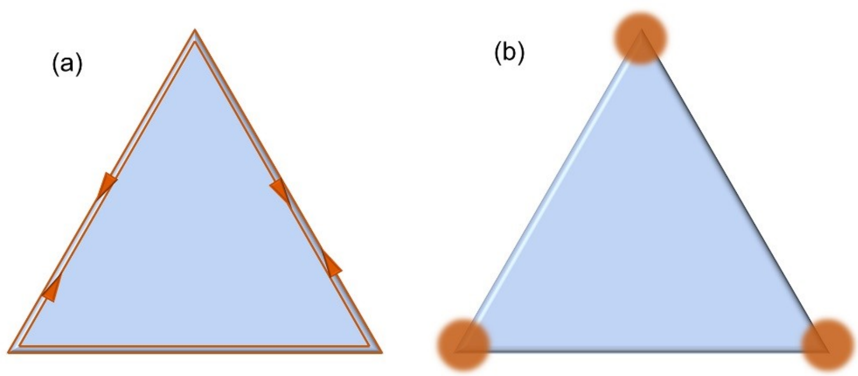

Fig. S7 (a) The schematic of carrier transport for conventional two-dimensional topological insulators, where carriers with opposite spins propagate in opposite directions along the edges, forming helical edge states. (b) The localized carrier distribution of higher-order topological insulators, where the carriers are confined to specific geometric locations.

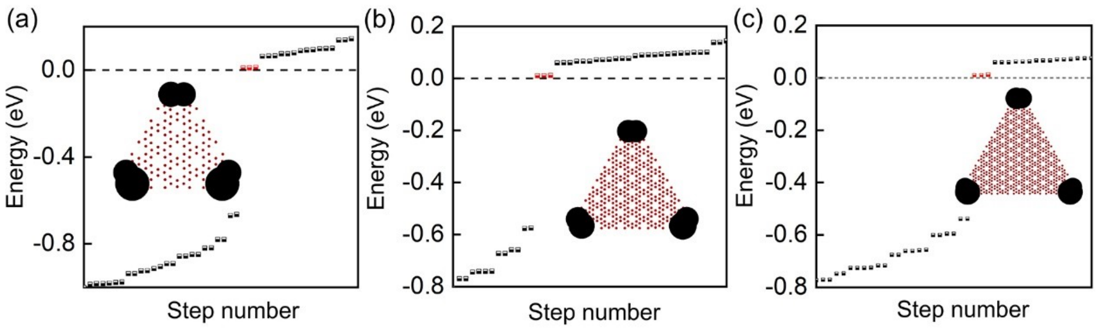

Fig. S8 Energy discrete spectra of the triangular nanoflakes for AFM CrI_3 monolayer with (a) 8×8, (b) 12×12 and (c) 16×16 sizes, where the bulk and nontrivial corner states are marked by red and black dots, respectively. Insets show the total charge distribution of the three occupied corner states.

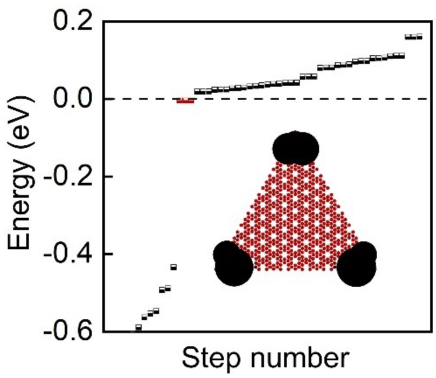

Fig. S9 Energy discrete spectrum of a nanoflake for FM CrI_3 monolayer without spin-orbital coupling. Red dots represent the in-gap corner states. Insets show the total charge distributions of the corresponding corner states.